

Breakdown of Elasticity in Amorphous Solids

Giulio Biroli^{1,2} and Pierfrancesco Urbani¹

¹*IPhT, Université Paris Saclay, CEA,*

CNRS, F-91191 Gif-sur-Yvette Cedex, France

²*LPS, Ecole Normale Supérieure, 24 rue Lhomond, 75231 Paris Cedex 05 - France.*

arXiv:1601.06724v1 [cond-mat.soft] 25 Jan 2016

What characterises a solid is its way to respond to external stresses. Ordered solids, such crystals, display an elastic regime followed by a plastic one, both well understood microscopically in terms of lattice distortion and dislocations. For amorphous solids the situation is instead less clear, and the microscopic understanding of the response to deformation and stress is a very active research topic. Several studies have revealed that even in the elastic regime the response is very jerky at low temperature, resembling very much the one of disordered magnetic materials. Here we show that in a very large class of amorphous solids this behaviour emerges by decreasing the temperature as a phase transition where standard elastic behaviour breaks down. At the transition all non-linear elastic moduli diverge and standard elasticity theory does not hold anymore. Below the transition the response to deformation becomes history and time-dependent.

Our work connects two different lines of research. The first focuses on the behaviour of amorphous solids at low temperature. With the aim of understanding the response of glasses to deformations, there have been extensive numerical studies of stress versus strain curves obtained by quenching model systems at zero temperature. One of the main outcome is that the increase of the stress is punctuated by sudden drops related to avalanche-like rearrangements both before and after the yielding point [1–5]. This behaviour makes the measurements, and even the definition of elastic moduli quite involved. In a series of works Procaccia et al. have given evidences that in some models of glasses, such as Lennard-Jones mixtures (and variants), non-linear elastic moduli display diverging fluctuations and linear elastic moduli differ depending on the way they are defined from the stress-strain curve [6, 7]. Another independent research stream has focused on the understanding of the jamming and glass transitions of hard spheres both from real space and mean-field theory perspectives [8, 9]. The exact solution obtained in the limit of infinite dimensions revealed that by increasing the pressure a hard sphere glass displays a transition within the solid phase, where multiple arrangements emerge as different competing solid phases [10, 11]. This is called Gardner transition in analogy with previous results in disordered spin models [12, 13]. Recent simulations have confirmed that in three dimensions these different arrangements become more and more long-lived, possibly leading to an ergodicity breaking [14]. These mean-field analysis complements and strengthens all the remarkable results found in the last two decades on jammed hard spheres glasses. The major outcome of these real space studies was the discovery that

amorphous jammed solids are marginally stable, i.e. characterised by soft-modes and critical behaviour and in consequence by properties which are very different from the ones of usual crystalline solids [15–17]. Within mean-field theory this is a consequence of a more general marginal stability emerging at the Gardner transition [9, 18].

Here we show that also models of structural glasses display this transition when decreasing the temperature and that this drastically affects their elastic behaviour. In particular, we reveal that elastic anomalies, such as the ones found in zero temperature simulations, are a signature of this phase transition. In order to show the existence and the properties of the Gardner transition in structural glasses we focus on a system of soft elastic spheres, which has been studied recently in several numerical simulations and shown to behave as canonical glass-formers [19–21]. The interaction potential between particles reads

$$\hat{V}_{\text{HSS}}(r) = \frac{V_0}{2} \left(1 - \frac{r}{\mathcal{D}}\right)^2 \theta\left(1 - \frac{r}{\mathcal{D}}\right) \quad (1)$$

where r is the distance between particles, V_0 is the interaction strength and \mathcal{D} the interaction range. We choose this model since in the limit $V_0 \rightarrow \infty$, it maps on hard spheres with diameter \mathcal{D} . This enables us to make connections with previous results on jamming.

In this work we want to study the elastic properties of amorphous solids created by thermal quenches and also by compression. Theoretically, these solids are actually ultra-viscous liquids observed on time-scales on which flow is absent. From the energy landscape perspective [22], these are systems unable to escape from a given metabasin within the experimental time-scale. The large dimensional limit ($d \rightarrow \infty$) is particularly useful to analyse these long-lived amorphous metastable states. Because the life-time of metastable states diverges exponentially with d , one does not have to develop a full dynamical treatment but can instead resort to a generalised thermodynamic framework able to capture the properties of metastable states [23]. What is generically considered a weakness of mean-field theory—the inability of describing activated dynamics in the super-cooled regime—becomes here an advantage. In the infinite dimensional limit meta-basins become very long-lived below a well defined temperature T_{MCT} , corresponding to the Mode Coupling Transition (MCT). Although in three dimensions the increase of the life-time of meta-basins is not as sharp below T_{MCT} (MCT becomes a cross-over), in the experimentally relevant regime we are interested in, amorphous solids do become well defined metastable states. Indeed, for realistic quenches (0.1-100 K/min), super-cooled liquids fall out of equilibrium at a temperature T_g

well below T_{MCT} , and their properties do not change with time (except on very large times where ageing sets in); hence, the generalised thermodynamic framework [23] we use is particularly adapted.

In order to solve the model (5) in the $d \rightarrow \infty$ limit and to study the properties of the metastable amorphous solids we use the replica method, whose order parameter is the mean square displacement between couples of replicas ($x_i^{(a)}$ is the position of the particle i in replica a):

$$\Delta_{ab} = \frac{d}{N\mathcal{D}^2} \sum_{i=1}^N \left| x_i^{(a)} - x_i^{(b)} \right|^2 \quad (2)$$

Roughly speaking, this order parameter allows to study the statistical properties of the metabasins and probe their ruggedness: a breaking of replica symmetry means that different replicas are trapped in different minima and, hence, that an ergodicity breaking transition has taken place within the solid phase. This method has been developed and explained in full detail in several recent works on hard spheres [24–26]. Hence, here we directly present our main results and refer to SM for the key technical steps (the whole derivation will be shown elsewhere [27]).

Henceforth we consider packing fractions such that $T_{MCT}(\varphi) > 0$ and focus on glass states formed by slow quenches below it ($T_{MCT}(\varphi)$ raises from zero at a well defined packing fraction φ which in three dimensions should correspond to $\varphi_{MCT} \simeq 0.58$). For a given cooling rate the system follows the equilibrium line in the energy-temperature plane until it falls out of equilibrium and becomes an amorphous solid at T_g . We have computed both the equilibrium and the amorphous solid branches, as shown in Fig.1 for a given packing fraction. The main results is that generically by decreasing the temperature amorphous solids undergo a Gardner transition at a temperature $T_G(\varphi)$. The lower is the glass transition temperature T_g the more one has to cool in order to reach $T_G(\varphi)$. By comparing the results obtained for amorphous solids formed at the same T_g at different packing fractions, we find that $T_G(\varphi)$ decreases when φ is augmented, as shown in Fig. 2 (for too small densities, when T_g crosses T_{MCT} , it is simply not possible to create a solid). We conclude this analysis by considering glasses formed by compression to make a relationship with studies on hard spheres and jamming. In this case, we find first a direct and then an inverse Gardner transition as shown in Fig. 3. The results obtained for glasses formed at the same φ_g at different temperatures show that the higher is the temperature the smaller is the extent of the Gardner phase, thus creating a

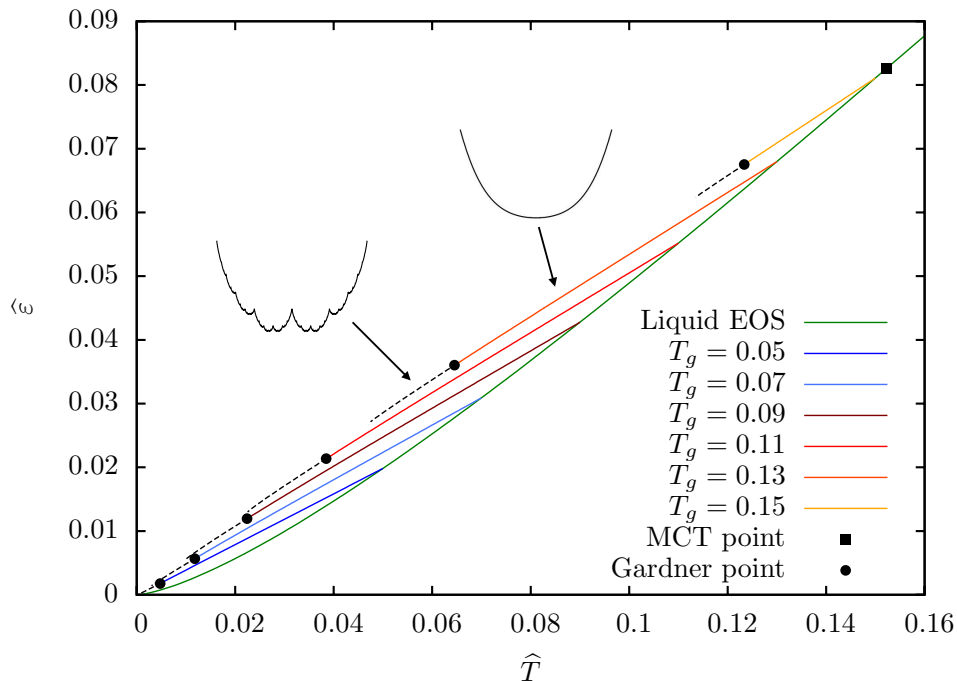


FIG. 1: Energy vs temperature (in rescaled units, see SM) for $\hat{\varphi} = \varphi 2^d/d = 8$. EOS denotes the equilibrium line obtained by the equation of state. The other lines correspond to amorphous solids created by different cooling rate (slower to higher from bottom to top). Lines become dashed when the Gardner transition takes place. The change in the free-energy landscape at the Gardner transition is shown pictorially.

dome in the $T - \varphi$ plane. This re-entrant behaviour is in agreement with very recent studies on the spectrum of harmonic vibrations of elastic sphere glasses [18, 28].

In summary, we have shown that amorphous solids undergo by cooling the same transition toward a marginal glass state found for hard spheres [11]. We can now turn to our main concern which is the change in the elastic properties of the solid approaching the Gardner transition. For a normal elastic solid, e.g. a crystal, a small shear strain γ induces a change in free energy per unit volume equal to

$$\frac{\mathcal{F}_{el}}{V} = \frac{\mu_2}{2}\gamma^2 + \frac{\mu_4}{4!}\gamma^4 + \dots \quad (3)$$

where V is the volume and μ_n is the n -th order elastic modulus: $\mu_n = \frac{d\sigma^{n-1}}{d^{n-1}\gamma}$ where σ is the stress (μ_2 is the usual linear shear modulus). This is also true for amorphous solids *but only above the Gardner transition*. Our explicit computation in the limit of infinite dimensions

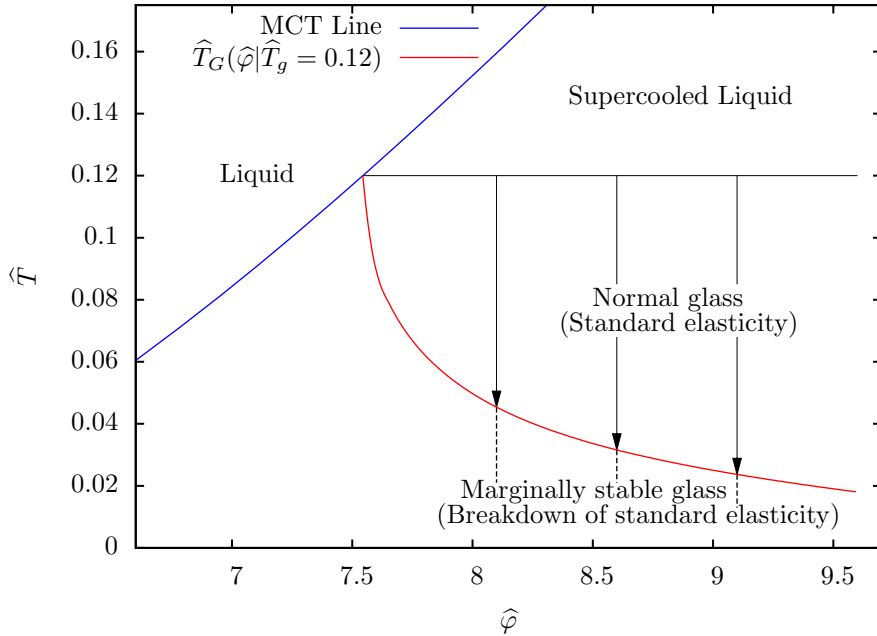


FIG. 2: Evolution of the Gardner transition temperature (red line) obtained by cooling amorphous solids at fixed φ . All amorphous solids are formed at the same $\hat{T}_g = 0.12$. The blue line denotes the MCT transition temperature as a function of $\hat{\varphi}$.

shows that in this regime all elastic moduli are well defined (up to fluctuations of the order $1/\sqrt{V}$) and that they depend on the glass state only through the value of T_g , i.e. the speed of the quench used to form the glass, and of the applied temperature and packing fraction [32]. The situation changes drastically approaching the Gardner transition line at which the fluctuations of all elastic moduli blow up. Although averages remain featureless, the fluctuations from one glass state to another, rescaled by their typical value $1/\sqrt{V}$, diverge as:

$$\overline{(\delta\mu_n\sqrt{V})^2} \sim \frac{1}{(T - T_G)^{2n-3}} \quad , \quad \overline{(\delta\mu_n\sqrt{V})^2} \sim \frac{1}{|\varphi - \varphi_G|^{2n-3}} \quad (4)$$

where the right and left expressions correspond to different protocols to induce the transition (cooling and compression). This increase leads to giant fluctuations at the Gardner transition. Finite size (mean-field) scaling implies that at the transition $\overline{(\delta\mu_n\sqrt{V})^2} \sim V^{2n/3-1}$. For $n = 2$ fluctuations are subleading, hence the linear elastic shear modulus is regular and well defined: $\mu_2 \simeq \bar{\mu}_2 + O(V^{-1/6})$. Instead all non-linear moduli are not: their fluctuations diverge as $V^{n/3-1}$ and completely overwhelm the average, which remains finite but is not representative of the typical behaviour. Note, moreover, that all odds moduli, that vanish

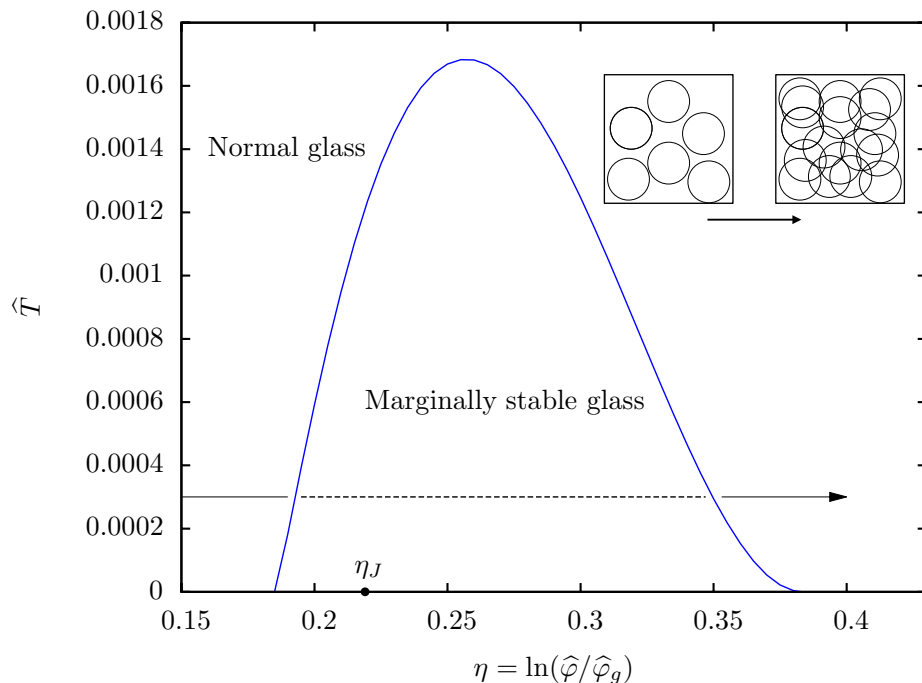


FIG. 3: Gardner critical packing fractions φ_G obtained by compressing amorphous solids at fixed temperature. All amorphous solids are formed at the same $\hat{\varphi}_g = 8$. The location of the jamming point is denoted by η_J .

by symmetry in ordered solids, can be neglected above T_G only. At T_G they also blow up and instead of being of the order of $1/\sqrt{V}$ (and zero in average) they diverge as $V^{n/3-1}$ and fluctuate. All these results signal that standard elastic behaviour breaks down at T_G . Below T_G , even an infinitesimal deformation leads in the thermodynamic limit to ageing and time-dependent shear moduli. In this regime, elastic moduli depend on the history and on the protocol used to measure them. Only strains whose amplitude scales to zero with V do not lead to ageing and irreversible behaviour [7]. The elastic moduli computed in this way, called quenched in [7] and zero-field cooled in [29], are a property of the meta-basin to which the system belongs. They are characterised by the same divergent fluctuations found at T_G . This is a consequence of the marginal stability of glasses within the whole Gardner phase. We derived our results in a specific realistic model in the limit of infinite dimensions. However, our findings go beyond the specific $d \rightarrow \infty$ computation we presented. Indeed one can obtain them using a Landau theory as shown in the supplementary material. Similarly to the existence of diverging magnetic responses at a ferromagnetic transition, the breakdown

of elastic behaviour and the divergence of non-linear elastic moduli are the generic signature of the Gardner transition [33].

In conclusion, our results unveil that the jerky elastic behaviour displayed by amorphous solids at low temperature could be related to the existence of a phase transition within the glass phase. Our exact solution in the limit of infinite dimensions characterises the dependence of this transition on the control parameters (T, φ) and protocols (cooling, compression), providing guidance for experimental tests both in structural, colloidal and possibly granular glasses. In order to substantiate our predictions, it is impelling to extensively study by experiments and by simulations whether standard elastic behaviour breaks down at a well defined temperature in the way identified in this work. The simulations of model systems quenched at zero temperature by Procaccia et al. display very promising results: the linear elastic intra-state modulus is found to be well defined, whereas μ_3 has fluctuations of $O(1)$ and μ_4 shows diverging fluctuations as we found. On the theoretical side, it is important to go beyond the Landau theory in order to obtain more quantitative predictions on the value of the critical exponents controlling the divergence of the elastic moduli. All that opens the way toward new research directions aimed at revealing the true nature of glasses. As suggested by several recent research results on jamming and amorphous plasticity, glasses might not be just liquids having stopped to flow but an entirely different new kind of solids [9, 30, 31].

Acknowledgments We thank J.-P. Bouchaud, P. Charbonneau, S. Franz, I. Procaccia, G. Tarjus, F. Zamponi for useful discussions. We acknowledge financial support from the ERC grant NPRGGLASS.

-
- [1] J.-L. Barrat and A. Lemaitre, in *Dynamical Heterogeneities in Glasses, Colloids, and Granular Media*, edited by L. Berthier, G. Biroli, J.-P. Bouchaud, L. Cipelletti, and W. van Saarloos (Oxford University Press, 2011).
 - [2] C. E. Maloney and A. Lemaître, *Physical Review E* **74**, 016118 (2006).
 - [3] A. Lemaître and C. Caroli, *Physical review letters* **103**, 065501 (2009).
 - [4] S. Karmakar, E. Lerner, and I. Procaccia, *Physical Review E* **82**, 055103 (2010).
 - [5] J. Lin, E. Lerner, A. Rosso, and M. Wyart, *Proceedings of the National Academy of Sciences*

- 111**, 14382 (2014).
- [6] H. G. E. Hentschel, S. Karmakar, E. Lerner, and I. Procaccia, *Physical Review E* **83**, 061101 (2011).
- [7] A. K. Dubey, I. Procaccia, C. Shor, and M. Singh, arXiv preprint arXiv:1512.03244 (2015).
- [8] A. J. Liu, S. R. Nagel, W. Van Saarloos, and M. Wyart, in *Dynamical Heterogeneities in Glasses, Colloids, and Granular Media*, edited by L. Berthier, G. Biroli, J.-P. Bouchaud, L. Cipelletti, and W. van Saarloos (Oxford University Press, 2011).
- [9] P. Charbonneau, J. Kurchan, G. Parisi, P. Urbani, and F. Zamponi, *Nature Communications* **5**, 3725 (2014).
- [10] J. Kurchan, G. Parisi, and F. Zamponi, *Journal of Statistical Mechanics: Theory and Experiment* **2012**, P10012 (2012).
- [11] J. Kurchan, G. Parisi, P. Urbani, and F. Zamponi, *J. Phys. Chem. B* **117**, 12979 (2013).
- [12] E. Gardner, *Nuclear Physics B* **257**, 747 (1985).
- [13] D. Gross, I. Kanter, and H. Sompolinsky, *Physical review letters* **55**, 304 (1985).
- [14] L. Berthier, P. Charbonneau, Y. Jin, G. Parisi, B. Seoane, and F. Zamponi, arXiv preprint arXiv:1511.04201 (2015).
- [15] C. S. O'Hern, L. E. Silbert, A. J. Liu, and S. R. Nagel, *Phys. Rev. E* **68**, 011306 (2003).
- [16] M. Wyart, S. Nagel, and T. Witten, *Europhysics Letters* **72**, 486 (2005).
- [17] M. Wyart, *Phys. Rev. Lett.* **109**, 125502 (2012).
- [18] S. Franz, G. Parisi, P. Urbani, and F. Zamponi, *Proceedings of the National Academy of Sciences* **112**, 14539 (2015).
- [19] L. Berthier and T. A. Witten, *Phys. Rev. E* **80**, 021502 (2009).
- [20] M. Schmiedeberg, T. K. Haxton, S. R. Nagel, and A. J. Liu, *EPL (Europhysics Letters)* **96**, 36010 (2011).
- [21] L. Berthier, G. Biroli, D. Coslovich, W. Kob, and C. Toninelli, *Physical Review E* **86**, 031502 (2012).
- [22] P. G. Debenedetti and F. H. Stillinger, *Nature* **410**, 259 (2001).
- [23] R. Monasson, *Phys. Rev. Lett.* **75**, 2847 (1995).
- [24] P. Charbonneau, J. Kurchan, G. Parisi, P. Urbani, and F. Zamponi, *Journal of Statistical Mechanics: Theory and Experiment* **2014**, P10009 (2014).
- [25] C. Rainone, P. Urbani, H. Yoshino, and F. Zamponi, *Phys. Rev. Lett.* **114**, 015701 (2015).

- [26] C. Rainone and P. Urbani, arXiv preprint arXiv:1512.00341 (2015).
- [27] G. Biroli and P. Urbani, In Preparation (2016).
- [28] P. Charbonneau, E. I. Corwin, G. Parisi, A. Poncet, and F. Zamponi, arXiv preprint arXiv:1512.09100 (2015).
- [29] D. Nakayama, H. Yoshino, and F. Zamponi, arXiv preprint arXiv:1512.06544 (2015).
- [30] C. P. Goodrich, A. J. Liu, and S. R. Nagel, *Nature Physics* **10**, 578 (2014).
- [31] G. Biroli, *Nature Physics* **10**, 555 (2014).
- [32] We are working in the NVT ensemble but of course our results can be translated to other cases, for example the more experimentally relevant NPT one.
- [33] As a matter of fact, our results also hold *mutatis mutandis* for spin-glasses in a field and provide new ways to test for the existence of the Almeida-Thouless line [27].

Supplementary material
Breakdown of elasticity in amorphous solids

Giulio Biroli and Pierfrancesco Urbani

I. INTRODUCTION

We consider a system of spheres interacting through a central potential $\hat{V}(r)$. A typical example is the Harmonic Soft Sphere interaction potential

$$\hat{V}_{\text{HSS}}(r) = \frac{V_0}{2} \left(1 - \frac{|r|}{\mathcal{D}}\right)^2 \theta\left(1 - \frac{|r|}{\mathcal{D}}\right) \quad (5)$$

where \mathcal{D} is the diameter of the sphere that fixes the interaction range and V_0 is the interaction strength. Taking the limit $V_0 \rightarrow \infty$ one gets back the Hard Sphere model. A glassy state α can be characterized by few control parameters such as the packing fraction φ and the inverse temperature β at which it is created, i.e. at which the super-cooled liquid fell out of equilibrium. We shall denote it $\alpha(\varphi, \beta)$. It can be thought as a metabasin of configuration of phase space that is explored ergodically for timescales shorter than the α -relaxation time. More precisely, we shall say that we *prepare* the system in a glass state $\alpha(\varphi_g, \beta_g)$ when the configurations that are sampled by the dynamics are equilibrium configurations of the metabasin to which the state α belongs to. Once a glassy state is prepared at a given point (φ_g, β_g) , we can look at how it changes when the control parameters are changed towards another state point (φ, β) . In particular we can compute the free energy of the glassy state once *followed* to this new state point and it is given by

$$f[\alpha(\varphi_g, \beta_g), \beta, \varphi] = -\frac{1}{\beta V} \ln \int_{X \in \alpha(\varphi_g, \beta_g)} dX e^{-\beta \mathcal{V}[X; \varphi]} \quad (6)$$

where $\mathcal{V}[X; \varphi] = \sum_{i < j} \hat{V}(|x_i - x_j|)$. The sum over the configurations X is done in such a way that they all belong to the same ergodic component characterizing the glass state $\alpha(\hat{\varphi}_g, \hat{\beta}_g)$. The packing fraction can be changed by changing the diameter of the spheres in (5), [1]. In order to compute the elastic response of the system we need to couple it to an external strain γ . In this way the interaction potential is changed due to the change in the shape of the box in which the system is placed. We denote the interaction potential in presence of the strain as $\mathcal{V}_\gamma[X; \varphi]$. If the shear strain is small, the change in the free energy (6) is given

by

$$V(f[\alpha(\varphi_g, \beta_g), \beta, \varphi; \gamma] - f[\alpha(\varphi_g, \beta_g), \beta, \varphi; 0]) = V\sigma\gamma + V\frac{\mu_2}{2}\gamma^2 + V\frac{\mu_3}{3!}\gamma^3 + V\frac{\mu_4}{4!}\gamma^4 + \dots \quad (7)$$

Since the amorphous state is a random structure we expect the elastic coefficients σ, μ_2, μ_3 and μ_4 to be random variables characterized by a proper probability distribution. From the expansion (7) it is clear that the shear stress is given by $df[\alpha(\varphi_g, \beta_g), \beta, \varphi; \gamma = 0]/d\gamma = \sigma$ while the shear modulus is μ_2 . The scaling in V in (7) can be deduced from extensivity. Moreover we expect that once we average the free energy over all glassy states $\alpha(\varphi_g, \beta_g)$, we get a function that is symmetric under $\gamma \rightarrow -\gamma$. This implies that

$$\overline{\sigma} = 0 \quad \overline{\mu_3} = 0 \quad (8)$$

where we have denoted with an overline the average over different glassy states $\alpha(\varphi_g, \beta_g)$. Conversely, the first moment of μ_2 and μ_4 is expected to be different from zero. If the glassy state $\alpha(\varphi_g, \beta_g)$ is followed up to a point that is close to a second order phase transition, like the Gardner point [2], we expect a dramatic change in the probability distribution of the elastic moduli, due to the presence of the soft modes developed at the transition.

II. FREE REPLICA SUM EXPANSION

Since we want to average over all glassy states α that can be found at (φ_g, β_g) we need to introduce replicas to handle the logarithm that appears in (6). In order to compute all the different cumulants it is very useful to consider each replica being subjected to a different strain γ . In this way we get s systems, each one subjected to a different shear strain γ_a . We thus define a replicated free energy

$$W[\varphi, \beta | \varphi_g, \beta_g; \{\gamma_a\}] = -\frac{1}{\beta V} \ln \overline{\prod_{a=1}^s \int_{X^{(a)} \in \alpha(\varphi_g, \beta_g)} dX^{(a)} e^{-\beta V \gamma_a [X^{(a)}; \varphi]}}. \quad (9)$$

Once the average over the glassy states $\alpha(\varphi_g, \beta_g)$ is taken, we end up with a replicated system of $s+1$ replicas [1, 3, 4] the first one being a representative configuration of the glass state planted at (φ_g, β_g) ; at the end we will consider the limit $s \rightarrow 0$. Note that the initial glass state at (φ_g, β_g) is unstrained so that $\gamma_1 = 0$.

If we expand this function around $\{\gamma_a = 0\}$ we get a free replica sum expansion [5, 6]

$$\begin{aligned}
W[\varphi, \beta|\varphi_g, \beta_g; \{\gamma_a\}] - W[\varphi, \beta|\varphi_g, \beta_g; \{\gamma_a = 0\}] &= \frac{\bar{\mu}_2}{2} \sum_{a=2}^{s+1} \gamma_a^2 - \frac{V\bar{\sigma}^{2c}}{2} \left(\sum_{a=2}^{s+1} \gamma_a \right)^2 \\
&- \frac{V^3\bar{\sigma}^{4c}}{4!} \left(\sum_{a=2}^{s+1} \gamma_a \right)^4 - \frac{V\bar{\sigma}\bar{\mu}_3^c}{3!} \left(\sum_{a=2}^{s+1} \gamma_a \right) \left(\sum_{a=2}^{s+1} \gamma_a^3 \right) - \frac{1}{8} V\bar{\mu}_2^{2c} \left(\sum_{a=2}^{s+1} \gamma_a^2 \right)^2 \\
&+ \bar{\sigma}^2 \bar{\mu}_2 V^{2c} \left(\sum_{a=2}^{s+1} \gamma_a \right)^2 \left(\sum_{a=2}^{s+1} \gamma_a^2 \right) + \frac{\bar{\mu}_4}{4!} \left(\sum_{a=2}^{s+1} \gamma_a^4 \right) + \dots
\end{aligned} \tag{10}$$

Due to extensivity, we have that $\bar{\sigma}^{2c} \sim 1/V$, $\bar{\sigma}^{4c} \sim 1/V^3$, $\bar{\mu}_2^{2c} \sim 1/V$, $\bar{\sigma}\bar{\mu}_3^c \sim 1/V$ and $\bar{\sigma}^2\bar{\mu}_2^c \sim 1/V^2$. Moreover, due to the symmetry $\{\gamma_a \rightarrow -\gamma_a\}$ we must have $\bar{\sigma}\bar{\mu}_2^c = 0$.

The replicated free energy (9) can be computed exactly in the infinite dimensional limit [1, 7] where we can carefully define metastable glassy states since nucleation and non-perturbative effects are highly suppressed. This is given in terms of an order parameter that is nothing but the distance between different replicas. If we denote as $x_i^{(a)}$ the position of the sphere i in replica a , we can define the mean square displacement (MSD) between couples of replicas as

$$\Delta_{ab} = \frac{d}{N\mathcal{D}^2} \sum_{i=1}^N \left| x_i^{(a)} - x_i^{(b)} \right|^2 \tag{11}$$

where d is the spatial dimension and it has been added in order to have a finite MSD matrix in the large dimensional limit. The matrix Δ_{ab} must be fixed by a saddle point equation $\partial W/\partial \Delta_{ab} = 0$. This means that the calculation of the cumulants in (10) can be done by expanding in powers of $\{\gamma_a\}$ the saddle point replicated free energy W . This is given by

$$W[\varphi, \beta|\varphi_g, \beta_g; \{\gamma_a\}] - W[\varphi, \beta|\varphi_g, \beta_g; \{\gamma_a = 0\}] = \frac{1}{2} \sum_{a,b=2}^{s+1} \mu_{ab} \gamma_a \gamma_b + \frac{1}{4!} \sum_{a,b,c,d=2}^{s+1} \chi_{abcd} \gamma_a \gamma_b \gamma_c \gamma_d + \dots \tag{12}$$

where

$$\begin{aligned}
\mu_{ab} &= \frac{dW}{d\gamma_a d\gamma_b} = \frac{\partial W}{\partial \gamma_a \partial \gamma_b} \tag{13} \\
\chi_{abcd} &= \frac{d^4 W}{d\gamma_a d\gamma_b d\gamma_c d\gamma_d} \Big|_{\{\gamma_a=0\}} = - \sum_{\alpha \neq \beta} \sum_{\mu \neq \nu} [M^{-1}]_{\alpha\beta; \mu\nu} [V_{\alpha\beta}^{ab} V_{\mu\nu}^{cd} + V_{\alpha\beta}^{ac} V_{\mu\nu}^{bd} + V_{\alpha\beta}^{ad} V_{\mu\nu}^{bc}] \\
&+ \frac{\partial^4 W}{\partial \gamma_a \partial \gamma_b \partial \gamma_c \partial \gamma_d} \Big|_{\{\gamma_a=0\}} \tag{14}
\end{aligned}$$

and where

$$V_{\alpha\beta}^{ab} = \frac{\partial^3 W}{\partial \gamma_a \partial \gamma_b \partial \Delta_{\alpha\beta}} \Big|_{\{\gamma_a=0\}} \tag{15}$$

$$M_{\alpha\beta;\mu\nu} = \frac{\partial^2 W}{\partial \Delta_{\alpha\beta} \partial \Delta_{\mu\nu}} \Big|_{\{\gamma_a=0\}}. \quad (16)$$

All the derivative are computed setting the order parameter Δ_{ab} to its saddle point value at $\{\gamma_a = 0\}$. From Eq.s (13-14) we see that the coefficients μ_{ab} are always regular while the quartic coefficients χ_{abcd} can develop divergencies due to the fact that the operator $M_{\alpha\beta;\mu\nu}$ can develop zero modes. This happens at the Gardner transition point [2]. The Gardner instability has been found in the context of the Hard Sphere model in [1, 2] and in the next section we will generalize these results to thermal systems. What we have done up to now is nothing but a Landau theory for the Gardner transition point.

In the normal glass phase, before reaching the Gardner instability, the saddle point MSD matrix has a 1-step replica symmetry breaking (1RSB) fashion (see the next section) and thus the form of the tensors M and V is simple. The tensor M has been discussed in [1, 2] while V is given by

$$V_{\alpha\beta}^{ab} = \delta_{ab} \left[\tilde{G}\Omega_{\alpha\beta}^a + \tilde{H}\Gamma_{\alpha\beta}^a \right] + (1 - \delta_{ab}) \left[\tilde{P}T_{ab;\alpha\beta}^1 + \tilde{Q}T_{ab;\alpha\beta}^2 + \tilde{R}T_{ab;\alpha\beta}^3 \right] \quad (17)$$

where the tensors Ω , Γ , T^1 , T^2 and T^3 are defined by

$$\begin{aligned} \Omega_{\alpha\beta}^a &= \frac{\delta_{a\alpha} + \delta_{a\beta}}{2} & \Gamma_{\alpha\beta}^a &= 1 & T_{ab;\alpha\beta}^1 &= \frac{\delta_{a\alpha}\delta_{b\beta} + \delta_{a\beta}\delta_{b\alpha}}{2} \\ T_{ab;\alpha\beta}^2 &= \frac{\delta_{a\alpha} + \delta_{b\beta} + \delta_{a\beta} + \delta_{b\alpha}}{4} & T_{ab;\alpha\beta}^3 &= 1. \end{aligned} \quad (18)$$

At the Gardner transition point the operator M develops a zero eigenvalue, the replicon, that we denote by λ_R . The corresponding eigenvector is a matrix $\delta_R \Delta_{ab}$ that satisfies the conditions

$$\begin{aligned} \sum_{a(\neq b)} \delta_R \Delta_{ab} &= \sum_{b(\neq a)} \delta_R \Delta_{ab} = 0 & a, b &= 2, \dots, s+1 \\ \delta_R \Delta_{1a} &= 0 & \forall a &= 2, s+1. \end{aligned} \quad (19)$$

This means that the first term on the right hand side of (14) can be divergent due to the zero mode. In order to evaluate the divergent parts of the cumulants in (10) we define the projector on the replicon subspace

$$P_{ab;cd}^{\parallel} = \frac{1}{2} (T_{ab;cd}^1 + T_{ab;cd}^2 + T_{ab;cd}^3) \quad a, b, c, d = 2, \dots, s+1 \quad (20)$$

and it is zero whenever one of the replica index is equal to 1. From the quartic derivatives we get that the singular part of the quartic derivative of the replicated free energy is given

by

$$\frac{d^4 W}{d\gamma_a d\gamma_b d\gamma_c d\gamma_d} \Big|_{\text{singular}} = -\frac{1}{\lambda_R} \sum_{(\alpha \neq \beta)(\mu \neq \nu)}^s P_{\alpha\beta;\mu\nu}^{\parallel} [V_{\alpha\beta}^{ab} V_{\mu\nu}^{cd} + V_{\alpha\beta}^{ac} V_{\mu\nu}^{bd} + V_{\alpha\beta}^{ad} V_{\mu\nu}^{bc}] \quad (21)$$

From this expression we finally get that the *divergent* part of the quartic cumulants of (10) is given by

$$\begin{aligned} V \overline{\sigma \mu_3^c} &= -\frac{3\tilde{P}^2}{2\lambda_R} \\ V \overline{\mu_2^c} &= \frac{3\tilde{P}^2}{2\lambda_R} \\ V^3 \overline{\sigma^4^c} &= \frac{3\tilde{P}^2}{2\lambda_R} \end{aligned} \quad (22)$$

The averages $\overline{\mu_4}$ and $V^2 \overline{\sigma^2 \mu_2^c}$ have no diverging contribution, i.e. they are finite at the transition. This is true for all $\overline{\mu_n}$. However, by going to higher orders in the free replica sum expansion we can get higher order correlation functions of the elastic moduli and in particular we can obtain the variances of the non-linear elastic moduli. These diverge as discussed in the text. The average finite values $\overline{\mu_n}$ are therefore not representative of the typical behaviour, which is dominated by the diverging fluctuations. As written in the main text, we have verified that these divergences, due to the vanishing of the replicon eigenvalue, also hold in the low temperature phase below T_G . All the detailed calculations will be presented elsewhere [8].

III. THE GARDNER TRANSITION IN THERMAL SYSTEMS

The Gardner transition that is responsible for the breakdown of the theory of elasticity in amorphous solids has been firstly detected in [1, 2] in the case of the Hard Sphere model. Here we want to generalize the theory to thermal systems. Let us consider a system of spheres that interact through an interaction potential of the following kind

$$\hat{V}(r) = \tilde{v} \left(d \left(\frac{|r|}{\mathcal{D}} - 1 \right) \right) \quad (23)$$

where \tilde{v} is a generic potential that decreases sufficiently fast at infinity [9]. The Harmonic Soft Sphere potential is exactly of this form. Indeed, in that case we have (we set $V_0 = 1$ without loss of generality)

$$\tilde{v}_{\text{HSS}}(h) = \frac{h^2}{2d^2} \theta(-h) = \frac{1}{d^2} v_{\text{HSS}}(h) \quad v_{\text{HSS}}(h) = \frac{h^2}{2} \theta(-h). \quad (24)$$

It is convenient to define a reduced temperature $\widehat{\beta} = \beta/d^2$ so that the Boltzmann factor becomes

$$e^{-\beta\widehat{V}_{\text{HSS}}(r)} = e^{-\widehat{\beta}v_{\text{HSS}}(h)}. \quad (25)$$

For a generic potential we will define $v(h)$ such that

$$e^{-\beta\widehat{V}(r)} = e^{-\widehat{\beta}v(h)} \quad (26)$$

where $\widehat{\beta}$ is an inverse temperature properly rescaled with the dimension.

We now consider the limit $d \rightarrow \infty$. In order to do that we need to consider scaled control parameters that are $\widehat{\beta}$ and $\widehat{\varphi} = 2^d\varphi/d$. By extending the calculations of [1, 10] we obtained the expression of the free energy of a glass state prepared at $(\widehat{\varphi}_g, \widehat{\beta}_g)$ and followed up to $(\widehat{\varphi} = \widehat{\varphi}_g e^\eta, \widehat{\beta})$. Within a fullRSB ansatz [7, 10], the order parameter Δ_{ab} is given by

$$\begin{aligned} \Delta_{1a} &= \Delta^r \quad \forall a = 2, \dots, s+1 \\ \Delta_{ab} &\rightarrow \{0, \Delta(x)\} \quad \forall a, b = 2, \dots, s+1 \quad x \in [0, 1] \end{aligned} \quad (27)$$

and the free energy of the glass state prepared at $(\widehat{\varphi}_g, \widehat{\beta}_g)$ and followed up to $(\widehat{\varphi} = \widehat{\varphi}_g e^\eta, \widehat{\beta})$ is given in by

$$\begin{aligned} -\beta f[\alpha(\varphi_g, \beta_g), \beta, \varphi] &= \frac{d}{2} + \frac{d}{2} \log \left(\frac{\pi \langle \Delta \rangle}{d^2} \right) - \frac{d}{2} \int_0^1 \frac{dy}{y^2} \log \left(\frac{\langle \Delta \rangle + [\Delta](y)}{\langle \Delta \rangle} \right) + \frac{d}{2} \frac{\Delta_R}{\langle \Delta \rangle} \\ &+ \frac{d\widehat{\varphi}_g}{2} \int_{-\infty}^{\infty} dh e^h g_{\Delta_R}(1, h + \Delta_R/2) f(0, h - \eta + \Delta(0)/2, \widehat{\beta}). \end{aligned} \quad (28)$$

where

$$\langle \Delta \rangle = \int_0^1 dx \Delta(x) \quad [\Delta](x) = x\Delta(x) - \int_0^x dy \Delta(y) \quad (29)$$

and where $\Delta_R = 2\Delta^r - \Delta(0)$. Moreover

$$g_\Lambda(1, x; \widehat{\beta}) = \int_{-\infty}^{\infty} \frac{dy}{\sqrt{2\pi\Lambda}} \exp \left[-\frac{y^2}{2\Lambda} - \widehat{\beta}v(x-y) \right] \quad (30)$$

while the function f together with $\Delta(x)$ and Δ^r satisfy the following saddle point equations

$$\begin{aligned}
f(1, h, \widehat{\beta}) &= g_{\Delta(1)}(1, h, \widehat{\beta}) \\
\frac{\partial f}{\partial x} &= \frac{1}{2} \frac{\dot{G}(x)}{x} \left[\frac{\partial^2 f}{\partial h^2} + x \left(\frac{\partial f}{\partial h} \right)^2 \right] \\
P(0, h) &= e^{h+\eta-\Delta(0)/2} g_{\Delta_R} \left(1, h + \eta - \frac{\Delta(0) + \Delta_R}{2}, \widehat{\beta}_g \right) \\
\dot{P}(x, h) &= -\frac{\dot{G}(x)}{2x} [P''(x, h) - 2x(P(x, h)f'(x, h))'] \\
\frac{1}{G(0)} &= -\frac{\widehat{\varphi}_g}{2} \int_{-\infty}^{\infty} dh P(0, h) (f''(0, h) + f'(0, h)) \\
\frac{\Delta_R}{G(0)^2} &= \frac{\widehat{\varphi}_g}{2} \int_{-\infty}^{\infty} dh P(0, h) (f'(0, h))^2 \\
\kappa(x) &= \frac{\widehat{\varphi}_g}{2} \int_{-\infty}^{\infty} dh P(x, h) (f'(x, h))^2 \\
\frac{1}{G(x)} &= \frac{1}{G(0)} + x\kappa(x) - \int_0^x dy \kappa(y) \quad x > 0 \\
G(x) = x\Delta(x) + \int_x^1 dz \Delta(z) &\iff \Delta(x) = \frac{G(x)}{x} - \int_x^1 \frac{dz}{z^2} G(z).
\end{aligned} \tag{31}$$

Before reaching the Gardner transition point, in the normal glass phase where standard elasticity holds, these equations are solved by a 1RSB ansatz that corresponds to putting $\Delta(x) = \Delta$ where Δ satisfies the much simpler set of equations

$$\begin{aligned}
\frac{2\Delta^r}{\Delta^2} - \frac{1}{\Delta} &= \widehat{\varphi}_g \int_{-\infty}^{\infty} dh e^h \frac{\partial}{\partial \Delta} \left[g_{2\Delta^r - \Delta} \left(1, h + \Delta^r - \Delta/2; \widehat{\beta}_g \right) \log g_{\Delta} \left(1, h - \eta + \Delta/2; \widehat{\beta} \right) \right] \\
0 &= \frac{2}{\Delta} + \widehat{\varphi}_g \int_{-\infty}^{\infty} dh e^h \left[\frac{\partial}{\partial \Delta^r} g_{2\Delta^r - \Delta} \left(1, h + \Delta^r - \Delta/2; \widehat{\beta}_g \right) \right] \log g_{\Delta} \left(1, h - \eta + \Delta/2; \widehat{\beta} \right)
\end{aligned} \tag{32}$$

The Gardner transition corresponds to the point where

$$0 = -1 + \frac{\widehat{\varphi}_g}{2} \Delta^2 \int_{-\infty}^{\infty} dh e^{h+\eta-\frac{\Delta}{2}} g_{\Delta_R} \left(1, h + \eta - \frac{\Delta(0) + \Delta_R}{2}, \widehat{\beta}_g \right) \left[\frac{\partial^2}{\partial \widehat{\beta}^2} \ln g_{\Delta}(1, h, \widehat{\beta}) \right]^2 \tag{33}$$

where the replicon eigenvalue vanishes. The rescaled energy of the system (in the infinite dimensional limit) at the 1RSB level is given by

$$\widehat{\varepsilon} = -\frac{\widehat{\varphi}_g}{2} \int_{-\infty}^{\infty} dh e^h g_{\Delta_R} \left(1, h + \frac{\Delta_R}{2}, \widehat{\beta}_g \right) \frac{\partial}{\partial \widehat{\beta}} \ln g_{\Delta} \left(1, h - \eta + \frac{\Delta}{2}, \widehat{\beta} \right) \tag{34}$$

Formulas (32), (33) and (34) have been solved and computed numerically to obtain the

phase diagrams of the main text. Their complete derivation with an extension of the theory with shear strain will be given elsewhere [8].

- [1] C. Rainone, P. Urbani, H. Yoshino, and F. Zamponi, *Phys. Rev. Lett.* **114**, 015701 (2015).
- [2] J. Kurchan, G. Parisi, P. Urbani, and F. Zamponi, *J. Phys. Chem. B* **117**, 12979 (2013).
- [3] S. Franz and G. Parisi, *Journal de Physique I* **5**, 1401 (1995).
- [4] A. Barrat, S. Franz, and G. Parisi, *Journal of Physics A: Mathematical and General* **30**, 5593 (1997).
- [5] P. Le Doussal, M. Müller, and K. J. Wiese, *Physical Review B* **77**, 064203 (2008).
- [6] G. Tarjus and M. Tissier, *Physical review letters* **93**, 267008 (2004).
- [7] P. Charbonneau, J. Kurchan, G. Parisi, P. Urbani, and F. Zamponi, *Journal of Statistical Mechanics: Theory and Experiment* **2014**, P10009 (2014).
- [8] G. Biroli and P. Urbani, In Preparation (2016).
- [9] J. Kurchan, T. Maimbourg, and F. Zamponi, arXiv preprint arXiv:1512.02186 (2015).
- [10] C. Rainone and P. Urbani, arXiv preprint arXiv:1512.00341 (2015).